Measures of Solar Diameter with Eclipses: Data Analysis, Problems and Perspectives

Costantino Sigismondi

Sapienza Università di Roma and ICRA, International Center for Relativistic Astrophysics
Piazzale Aldo Moro 5, 00185 Roma Italia email: sigismondi@icra.it

Abstract. The theme of solar diameter variability is presented with the data of solar astrolabes, the four data points of the Solar Disk Sextant and the central eclipses observed near the shadow's limbs. All data are from the last 3 decades. The results obtained with solar astrolabes are different from Northern (Calern) and Southern hemisphere (Rio de Janeiro, Santiago), this is possibly due to atmospheric effect. Eclipses measurements are not affected by atmospheric turbulence because the event's geometry is determined outside the atmosphere, they give systematically larger diameter values than astrolabes. Videos of eclipses are discussed in term of projection on a screen versus direct imaging at the focal plane with filtered telescope. Relations between filters densities, telescope diameters, frame rate of video cameras, and portion of the outer solar limb lost during eclipse imaging are presented. Loss of 0.02" are typical for 10 cm ND5 filtered telescope. A commercial 60 fps camcorder for Baily beads timing is discussed in terms of signal-to-noise ratio.

Keywords: Eclispes; Ephemerides; Astrometry; Solar Physics; Diameter; Photosphere; Solar Variability.
PACS: 95.10.Gi; 95.10.Km; 95.10.Jk; 96.60.-j; 96.60.Bn; 96.60.Mz; 92.70.Qr.

SOLAR DIAMETER VARIATIONS

The question of solar secular variability remains still controversial after more than three decades of debate (Eddy and Boornazian 1979, Thuillier, Sofia, Haberreiter 2005). The 11 years cycle show up on Astrolabes measurements and markedly on the measurements made by Francis Laclare (from 1975 to 2006) on the plateau of Calern (Observatoire de la Côte d'Azur, France). There are also measurements made at the astrolabes of Rio de Janeiro and São Paulo, covering a minor time span. From 1925 to now there is an overall decrease of solar radius ΔR=-0.50" observed with eclipses.

FIGURE 1. Measurements of solar radius at the Astrolabe of Calern made by a single observer, Francis Laclare from 1975 to 2006. Data are averaged on groups of 40. The complete sequence consists of 7280 observations. The periodicity of 11 years is put into evidence by the time grid. While the amplitude of such 11 years oscillations is reducing with time, the linear trend (black line) is rising.. Each value is reduced at the same zenithal distance of z=0°. Such measurements are visual, with an impersonal astrolabe of Danjon. The use of a CCD in the last decade has confirmed the trend of visual measurements (Laclare et al. 1999). The diameters have been measured by timing transits on almucantarats, i.e. circles of equal height above the horizon, sampling helioghraphic latitudes between 15° and 90°, while at Rio de Janeiro, Santiago de Chile and São Paulo the equatorial zone can be sampled.

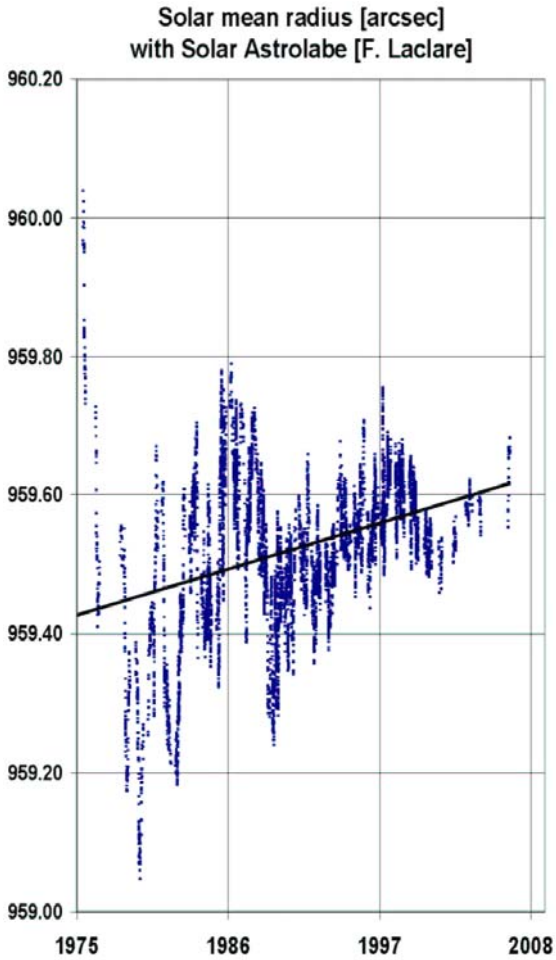

FIGURE 1. Data: Courtesy of Francis Laclare.

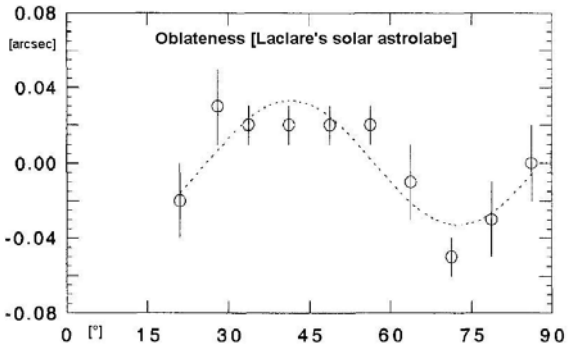

FIGURE 2. From Laclare et al. 1999. Residuals from mean radius [arcsecs] plotted as function of heliographic latitudes [°]. The latitude of Calern observatory, φ=43.5°, does not allow to have transits of the solar equator across the selected *almucantarats*, while the "royal zone" around 40°, where sunspots develop, is well sampled. An excess of 0.04" over 1919.26" yields an oblateness of $2 \cdot 10^{-5}$ twice larger than the upper limit measured during the four SDS, Solar Disk Sextant, flights (Egidi et al. 2006).

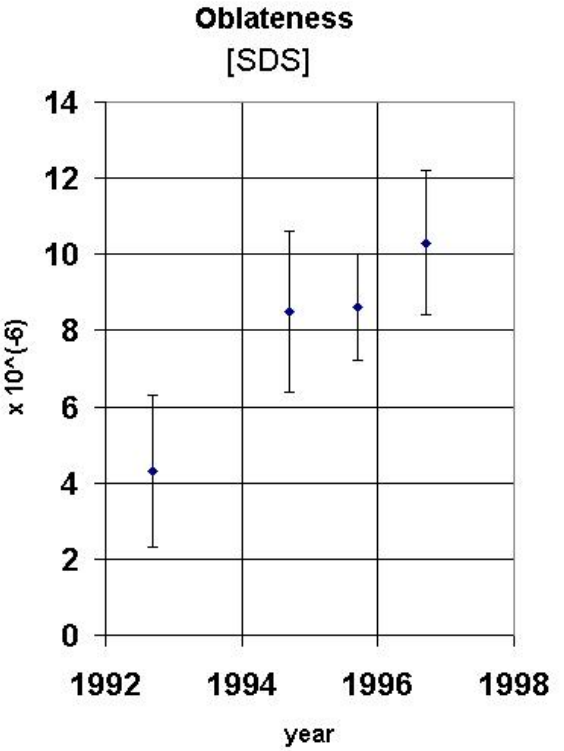

FIGURE 3. Oblateness vs time from SDS measurements (data plotted from Egidi et al., 2006).

The controversy among data obtained at different astrolabes appears in the comparison made by Noel (2004), even if the values of solar diameters plotted in figure 4 are not referred to the same heliographic latitude.

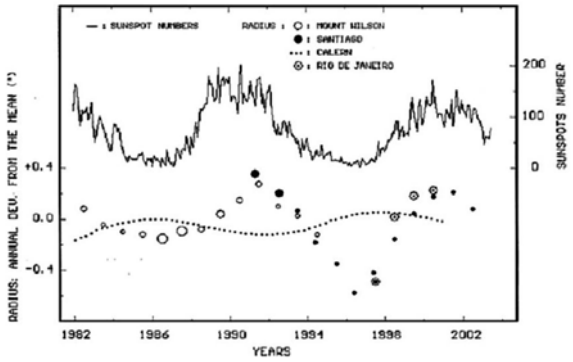

FIGURE 4. From Noel (2004) Mount Wilson observations (open circles) are added to Santiago measurements (filled circles) to cover the duration of Laclare's series. The measurements of Santiago, Mount Wilson and Rio de Janeiro follow an oscillation in phase with solar activity (upper curve). The series of Laclare is in anti-phase.

Atmospheric influence on diameter measurement

A local effect due to the atmosphere, different from each observatory location, with the solar cycle as principal forcing is also possible. Some periodical winds, related to the optical turbulence, are zonal, and inverse situation for Northern and Southern hemisphere are reasonably expected. Nevertheless no definitive explanation for this difference is still accepted. All systematic effects on those measurements are still to be clarified.

Solar 11 years influence on the atmosphere

Analyzing many lunar total eclipses, Danjon has shown that the brightness of eclipsed Moon [in Danjon scale] is maximum at maximum solar activity and minimum at minimum activity. Then solar activity influences our atmosphere through which the red rays are refracted toward the eclipsed Moon.

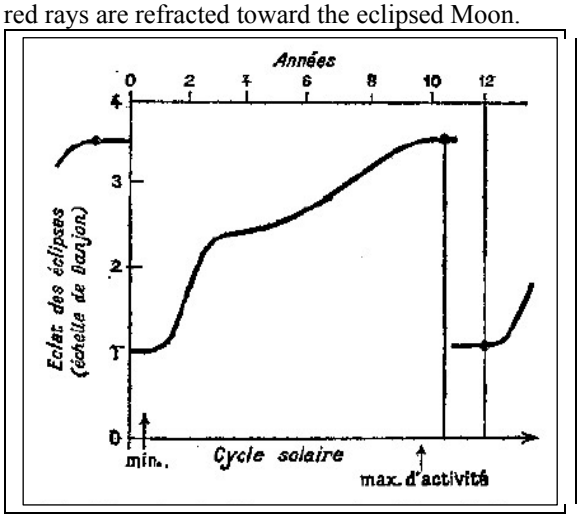

FIGURE 5. From Couderc (1971). Luminosity of lunar total eclipses in the Danjon scale as function of solar cycle.

ECLIPSE MEASUREMENTS

Evidences of secular changes comes from eclipse measurements (starting with 1715 Halley's eclipse in London, with a flashback in 1567 for the puzzling Clavius' annular total eclipse observed in Rome) and Mercury transits durations.

The more recent eclipse measurement with complete analysis available now (August 27, 2008) is the annular eclipse of September 22, 2006 (French Guyana). The eclipse was observed on centerline with 13 identified beads and Δt=0.04 s (Sigismondi, 2008).

The correction to standard mean solar radius 959.63" at unit distance is ΔR=0.07"±0.06" without Morrison and Appleby (1981) corrections.

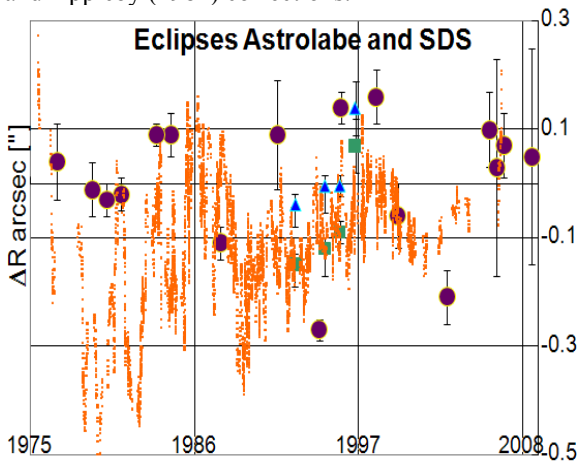

FIGURE 6. Corrections [arcsec] to mean solar standard radius of 959.63": comparison between eclipse measurements of solar radius, astrolabe and SDS in the last three decades. The eclipse data are taken from Dunham et al. 2005, the last eclipses from Sigismondi 2006 and 2008a;b. Black circles represent data of eclipses. Dots are astrolabe visual data from Francis Laclare. SDS data are represented with triangles (2008 analysis, from Djafer et al.) and with squares (2006 analysis from Egidi et al.). Between the two analysis there is a difference of 0.1". The agreement with Laclare's homogeneus visual data is in the local rising trend, while the annular eclipse of May 10, 1994 yields a radius which is much smaller than SDS and astrolabe measurements. The reason could be found in the filter used during the video record of such eclipse. The last eclipse has been observed with 7 cm with projection on screen. Other eclipses published do not have filters indications and consequently no systematic corrections. Videos with projected Sun during eclipses see beads longer than filtered telescopes, ΔR is closer to real value.
Data on annular eclipse of Spain 2005 and total eclipse of Egypt 2006 and China 2008 are included in this plot without Morrison and Appleby (1981) corrections; the last two total eclipses need still more analysis because only the duration of totality is available on the northern limit, with some uncertainty on the observer's position.

HISTORICAL ECLIPSES

Simulations on April 9, 1567 eclipse (Eddy and Boornazian, 1979 and Stephenson, Jones and Morrison, 1997), that Clavius (1581) observed as annular, opened the astrophysical question about secular solar radius variations.

For 1715 and 1925 eclipses the observed durations of totality and the corresponding locations have been used to locate two opposite umbral limits.

With precise ephemerides (Herald's winoccult software, 2007) the solar radius fitting better the data is evaluated and reduced to unit distance.

Baily Beads timing

During a central eclipse Baily beads are produced by the light from solar limb passing through lunar valleys of lunar limb. Baily beads timing technique associate to a single eclipse N data, and improves the statistical accuracy of a factor √N.

$\Delta R=0.16''(13/N)^{0.5}\cdot(\Delta t/0.025s)$, where Δt is the frame rate.

In 1979 data consisted on videos of 47 Baily beads events (instant of light ON or OFF through lunar valleys), all UTC referred, with geographical location of the observers very well known.

TABLE 1. Corrections to average solar radius at uniy distance (959.63") from Fiala et al. (1994) and from Sigismondi et al. *(2008, this volume).

Date	Type of Eclipse	Correction to solar radius
May 3 1715	*Total 3 obs.*	*ΔR=(+0.48±0.20)*
May 5 1832*	*Mercury tr.*	*ΔR=(+0.77±0.10)*
Aug 7 1869*	*Total 3 obs*	*ΔR=(+0.23±0.20)*
Jan 24 1925	*Total 8 obs.*	*ΔR=(+0.51±0.08)*
Feb 26 1979	*Total 47 obs*	*ΔR=(-0.11±0.05)*

The eclipses of 1925 and 1979 are separated by three SAROS cycles, so the Baily beads of the eclipses are produced by the same lunar limb features. This property of SAROS cycle has been used to improve eclipse data (Dunham 2005).

There is a secular shrinking of solar diameter from 1715 to 1979, mostly in the last 54 years.

There is still a random-like error smaller than 0.2" on the profile of single lunar features: that error is reduced enlarging the number N of Beads.

The technique introduced by Dunham of using polar beads, since the latitude libration of the Moon is near 0 during eclipses {the Moon is actually on the ecliptic during the eclipse} consists therefore to compare the same beads in different eclipses. Same beads in different eclipses implies that the random-like error becomes systematic and small differences between solar radius become visible at a level of 0.02"/0.05" of accuracy.

Atmospheric turbulence

The eclipse geometry is determined outside the atmosphere and local turbulence does not affect the timing of Baily beads events (instant of apparition or disappearing).

Even very bad seeing conditions of 5 arcsecs correspond to a Fried parameter r_0=2 cm, which is the aperture of a diffraction limited telescope, allowing the maximum angular resolution of 5".

Any larger telescope would produce speckles of coherence time around 1 ms, typical of optical turbulence. Long exposures are longer than 7/10 times this coherence time, the short ones below this limit.

The image of a point like bead is spread on 5" for long exposures, while it is made of speckles of the diffraction size for short exposures. Videos at frame rates of 25 fps and 60 fps are made by short exposure single frames.

OBSERVATIONAL EQUIPMENT

The paths of total eclipses are seldom on astronomical observatories, so the technical equipment has to be light enough to go on the carry-on baggage in airplanes. Until now telescopes of 7-12 cm of diameter and videocameras with CCD sensors at 1/25 s, with GPS were used in eclipse mission. Now total eclipses (better signal-to-noise ratio in the projected image) can guarantee to video-record N~50 Baily Beads, with Δt=1/60s.

Since $\Delta R \propto 1/(\sqrt{N}\cdot\Delta t)$, with respect to annular eclipse of 2006 we expect a factor of 4 of improvement in accuracy (N from 13 to 50 and Δt from 1/25 to 1/60) with $\sigma\Delta R$ from 0.16" to 0.04".

Telescope

The telescope already used for French Guyane annular eclipse of September 22, 2006, is a MEADE ETX70, 7 cm aperture, electronic altazimuth mount. The diameter is comparable with Fried parameter r_0 expected during the eclipse, so the pixel size of ~3 arcsec will match the effective angular resolution of the telescope with atmospheric turbulence.

In our studies on Spanish annular eclipse of 2005 videos of Baily beads taken with 20 cm telescopes are worse than with smaller ones.

Limiting Magnitude, Filtering and Projection

The observation of Baily beads during total eclipses is made in two ways: by projection on a screen or placing the detector at the primary focus of the telescope filtered by a ND4 or ND5 solar filter.

ND4 transmittance is $t=10^{-4}$, with a loss of 10 magnitudes. ND5 filter has $t= 10^{-5}$, corresponding to a 12.5 magnitudes drop.

Telescope's aperture, detector's sensitivity at video's frame rate and Limb Darkening Function determines the limiting magnitude detectable.

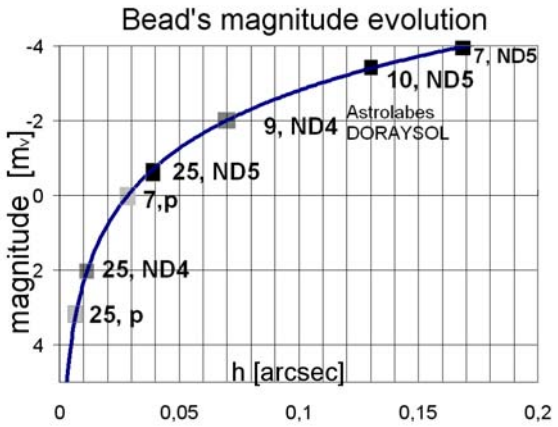

FIGURE 7. The magnitude mv of a Baily bead is calculated with Limb Darkening Function tabulated by Rogerson (1959) and it is represented as function of its depth [arcsec]. The magnitude for the full disk of radius 959.63" is mv=-26.4. Baily bead's area is ½ h^2, with h the dept in arcsec plotted in the figure. From this figure is evaluated the amount of solar limb cut out by the various filters. The luminosity [mV] of a bead depends on solar limb darkening function and it The whole Sun is mV =-26.4. The last bead detectable for 7, 9, 10 and 25 cm telescope is shown by projection on a screen (p) and with ND4 (10^{-4} transmittance, used for DORAYSOL) and ND5 ($t=10^{-5}$, used for Laclare's Astrolabe). The corresponding depth h is the perceived solar limb correction (negative) which is not real.

For MEADE ETX70, the limiting magnitude for point like sources (not planets), using the naked eye as detector is mv≤-4 with ND5 filter. In the case of projection on a white screen at 10 cm from the eyepiece in a dark environment the limiting magnitude is mv=0 (test made with Arcturus). A Baily bead is of magnitude mv=0 when its dept h=0.03", while it is of mv=-4 with h=0.17". All beads formed in the last 0.17" of photosphere are lost with (7, ND5) combination of telescope + filter, therefore the perceived solar limb has a ΔR=-0.17": correction which is not real, but systematic.

For (7, p) ΔR=-0.03".

CMOS sensor at 60 fps

I have tested a commercial videocamera SANYO CG9 with 1/60s frame rate CMOS sensor, giving a resolution of 640x480 pixel.

Being the angular diameter of Sun and Moon around 2000", we have 4" per pixel, if the whole disk fills the field of the camera.

Preparing the observation with opportune simulation is possible to select one part of the image, that one interested by Baily beads, and obtain better angular resolutions.

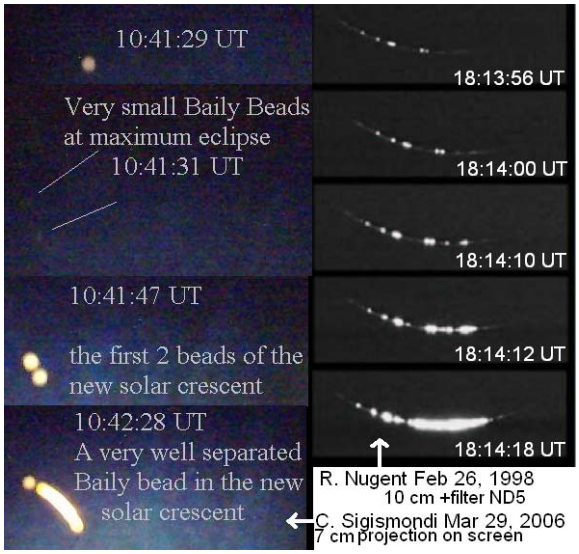

FIGURE 8. Images of Baily beads from two videorecords: left obtained by projection with MEADE ETX70 during the total eclipse of March, 29 2006 in Egypt; right through ND5 filter and 4 inches telescope by Richard Nugent at Curaçao on February 26, 1998. The images of left are out of focus, but the signal light ON/OFF is unambiguous.

In order to determine the limiting magnitude with that detector coupled with MEADE ETX70 7 cm refracting telescope f/5, I have observed the projection of the Moon on a screen.

With 60 fps (exposure times of 1/60 s), the contrast between lunar Maria and brighter surface is detectable when the full Moon projection is 4 cm of diameter.

With the eye (which has an integration time approximately 6 times larger, 1/10 s) the contrast is detected until the image reaches 8 cm of diameter, i.e. 1.5 magnitudes less bright. Consequently the limiting magnitude of the system 7 cm telescope + white projecting screen + CMOS detector at 60 fps is mv=-1.5 (0 being the limit for point like source detected by the naked eye).

In this way the last 0.056"of solar limb are not seen by this system (7,p+CMOS 60 fps). ΔR=-0.056" systematic.

In the case of traditional CCD at 25 fps the integration time is 2.4 larger and the limiting magnitude becomes, following the Pogson law:

$2.5 \cdot \log(2.4)=0.95$ brighter, i.e. mv=-0.55;

and that corresponds to ΔR=-0.036" systematic.

For a 10 cm telescope like MEADE 2045D with ND5 filter and 25 fps CCD ΔR=-0.02" systematic.

Signal-to-noise ratio

The size of the projected image of the Sun is typically 12 cm.

For the full Moon the larger projected and detected diameter was 4 cm, with a limiting surface brightness of mv=-13.6 (full Moon luminosity) over 50 cm², i.e. -9.35 magn/cm².

In the case of Baily beads with a solar diameter projected of 12 cm we have 16.2% of mv=-26.4 magnitudes (luminosity at solar limb with respect to central luminosity, according to Rogerson, 1959) over 452 cm², i.e. -17.78 magn/cm². The luminosity of Baily beads is large enough to be detected at 60 fps with an ideal signal-to-noise ratio.

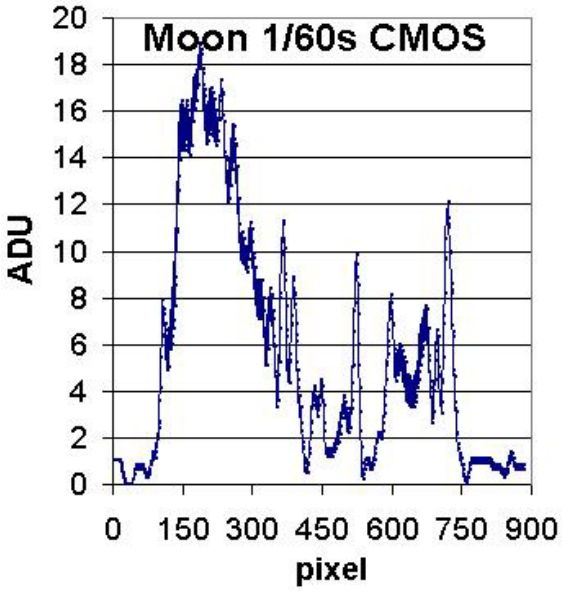

FIGURE 9. The background B in this image is from pixel 0 to 100 and 750 to 900, and the noise is σB=0.9 ADU. The brighter parts of the lunar surface show a signal-to-noise ratio larger than 20.

The environmental luminosity during the observation of the Moon reported in figure 9, which determines the background luminosity and then the noise in the projection method, has been estimated

similar to the total solar eclipse case, because the solar corona is 10^{-5} of the luminosity of the solar disk, and it is comparable to that one of the full Moon. Moreover Rome's city lights reproduce the environmental luminosity of the sky near the horizon during a total eclipse.

CONCLUSIONS

An observational campaign of grazing eclipses need always an international coordination, possible through the President of IOTA (International Occultation Timing Association), David W. Dunham (Johns Hopkins University Applied Physics Labs). It is important to assure that skilled observers go both to the Northern and Southern limits of the eclipse, with scientifically relevant observations, in order to rise the probability of successful Baily beads timings, good also to evaluate possible ephemeris errors in lunar latitude at 1/100" level.

The methods of solar diameter measurement with astrolabes using solar transits on fixed *almucantarats* (equal height circles) or the drift-scan method (transits on hourly circles) have to match the eclipse data which are the more accurate possible from the Earth. The observation of the next total eclipses (July 22, 2009) will give a precise reference of actual solar radius (at the beginning of Cycle 24) at unit distance for calibrating all instruments and methods. According to the hypothesis of inverse proportion between diameter and number of solar spots the diameter of the Sun in this time would be larger than in all other phases of the solar cycle during which PICARD satellite will fly (after June 2009). The mission is named PICARD after the pioneering work of Jean Picard (1620-1682) who precisely determined the solar diameter during the Maunder minimum.

GPS measurements error are on the 2/3 meters scale, unless DGPS or long integration time is used.

With a eclipse path width of 300 km an error of 3 m corresponds to one part in 10^5, which is 0.02" in solar radius correction.

Even the errorbar of SDS (Egidi et al., 2006) measurements is ±0.05", larger than the expected one ($\sigma\Delta R$=0.04") for these eclipses.

The results from the next eclipses are useful and accurate reference point for daily monitoring of solar diameter with astrolabes, as well as to semiperiodical monitoring, as the eclipse sampling is.

Acknowledgments: Thanks to David W. Dunham and to IOTA observers for sharing last eclipse data. Thanks to ICRANet for granting my observations of 2006 eclipses (annular in Guyana and total in Egypt).

REFERENCES

1. Clavius, C., *Commentarius in Sphaeram*, Venezia (1581²)
2. Dunham D.W., Sofia S., Fiala A.D., Muller P.M., Herald, D., *Observations of a probable change in the solar radius between 1715 and 1979*, Science **210**, 1243–1245 (1980).
3. Dunham D. W. et al., *Accuracy of Solar Radius Determinations from Solar Eclipse Observations, and Comparison with SOHO Data*, 2005 SORCE Science Meeting September 14-16, Durango, Colorado. (2005).
4. Eddy, J.A. and A. A. Boorrnazian, Bull. Am. Astron. Soc. **11**, 437 (1979).
5. Egidi, A., B. Caccin et al., *High-Precision Measurements of the Solar Diameter and Oblateness* by the Solar Disk Sextant (SDS) Experiment, Solar Physics **235**, 407–418 (2006).
6. Djafer, D., G. Thuillier, S. Sofia, A. Egidi., *Processing Method Effects on Solar Diameter Measurements: Use of Data Gathered by the Solar Disk Sextant*, Solar
7. Fiala, A.D.; Dunham, D. W.; Sofia, S., *Variation of the Solar Diameter from Solar Eclipse Observations*, 1715-1991, Solar Physics **152**, 97-104 (1994).
8. Herald, D., *WinOccult 3.1.0-3.6* http://www.lunar-occultations.com/iota/occult3.htm (2001-2006)
9. Rogerson, B.D., *The Solar Limb Intensity Profile*, Astrophysical Journal **130**, 985 (1959).
10. Stephenson, F. R., J. E. Jones, and L.V. Morrison, *The solar eclipse observed by Clavius in A.D. 1567*, Astronomy and Astrophysics **322**, 347-351 (1997).
11. Thuillier, G., S. Sofia and M. Haberreiter, *Past, Present and Future Measurements of the Solar Diameter*, Advances in Space Research **35** 329–340 (2005).
12. Couderc, P., *Les Éclipses*, Presses Universitaires de France, Paris (1971).
13. Noel, F., *Solar cycle of the apparent radius of the Sun*, Astronomy and Astrophysics **413**, 725-732 (2004).
14. Laclare, , F., Delmas, C. and A. Irbah, A., *Variations apparentes du rayon solaire observées à l'observatoire de la Côte d'Azur (Astrolabe solaire du site de Calern: 1975–1998).* C R. Acad. Sci. Paris 327 (Series II b), 1107-1114, (1999).
15. C. Sigismondi, C., *Solar Radius Variations Measured in Central Eclipses*, AIP Conf. proc. **966**, 341-8 (2008).
16. C. Sigismondi, C., *Solar radius in 2005 and 2006 eclipses*, IAU **233** Colloquium Proc. , 519-520 (2006).
17. Assus, P.; Irbah, A.; Bourget, P.; Corbard, T.; the PICARD team, Monitoring the scale factor of the PICARD SODISM instrument, Astronomische Nachrichten , **329**, p.517 (2008).
18. Rogerson, B.D., *The Solar Limb Intensity Profile*, Astrophysical Journal **130**, 985 (1959).
19. Sigismondi, C., M. Bianda and J. Arnaud, *European Projects of Solar Diameter Monitoring*, Proc. of V Sino-Italian Workshop, AIP, this volume, (2008).
20. Morrison, L. V. and G. M. Appleby, *Analysis of Lunar Occultations. III Systematic Corrections to Watts' limb-profiles for the Moon*, Mon. Not. R. Astron. Soc. **196** 1013-1020 (1981).